World Applied Sciences Journal 7 (4): 485-497, 2009
ISSN 1818-4952

Single Slope Solar Still for Sea Water Distillation

S.M. Radwan, A.A. Hassanain and M.A. Abu-Zeid

Agriculture Engineering Department, Faculty of Agriculture,
Suez-Canal University, Ismailia, 42552 Egypt

Abstract: Investigations were carried out under the open environmental conditions of Egypt on single slope solar still inclined 20° of one direction (I-20°OD). The experimental unit's composed three main components: solar distillation unit water leveling unit and preheating feeding tank. The solar distillation unit consists of two main components: transparent glazing cover of 0.006 m thickness and steel basin. The steel basin had dimension of 0.80 m length, 0.50 m width, 0.10 m height and 0.002 m thickness. Within these investigations the absorbing material type was matt black fiberglass and the basin water depth was kept at 0.5 cm (i.e. 2 liter). Basin was fed by the Suez Canal saline water. Meanwhile, volume of saline water was measured by grading container while distilled water was measured by measured vessel via a tilted channel fitted on unit sides. The investigation addressed the following: The still productivity, distilled water salinity and still performance in terms of the still efficiency (η) and. the coefficient of performance (C.O.P). Heat losses from the solar still were also considered. The highest still average productivity was obtained at August compared to May, June and July, as no productivity was obtained on June.

Key words: Inclined solar still · Sea water distillation · Still productivity · Performance · Efficiency and heat losses

INTRODUCTION

Water and energy are the two basic elements that influence the quality of civilized life. Fresh water is the fundamental life source on earth. Water consumption is increasing all over the world due to the rapid increase of population and the agricultural explosion projects. This causes a serious demand on the fresh water. Around twenty five percent of the world population lives in arid or semi-arid areas with lack of fresh water supply [1]. Most of the total water resources comes from Nile River (Ninty percent) it is about 850 cubic meters per year in Egypt, which places it below the "water poverty level" (1,000 m^3/year) accepted by the World Bank [2] in Egypt. Distillation is one of the most important factors that can assist in the remote and areas under developing. Water desalination can be accomplished by different techniques that can be classified under two categories [3], the membrane processes such as reveres osmosis and electrodialysis. Meanwhile, thermal processes such as multi stage flash distillation, multi effect boiling, vapor compression and solar distillation.

Solar Distillation is particularly important for locations where solar intensity is high and there is a scarcity of fresh water classified into: direct (passive) and indirect (active) regimes. The direct solar distillation systems collect solar energy to produce the stilled water directly compared to the indirect systems categories. passive solar stills is recommended as it is economical to provide potable water and active solar distillation system from a commercial point of view compared to the active stills [4,5].

Abdel-Ghafar [6] investigated a passive solar basin still type in Alexandria, Egypt. The still was fabricated from simple available materials (i.e. wood, corks, galvanized steel, glass pane and mirrors). The still was sloped by 30°; it was oriented toward the south direction. It had area of 1.2 m^2 with a projected area of 1.1 m^2. A mirror of 0.7 m^2 was fitted on the still side walls. The maximum obtained basin water temperatures were found 53°C and 56°C at the experiments in June and July, respectively as the distilled water of 2 liter/m^2.day was obtained.

Fath *et al.* [7] found that the single slope still was slightly more efficient than the pyramid-shape one. The solar energy received by the single slope still was 8% higher than that received by the pyramid in winter while it was 5% lower in summer. Due to the larger radiation losses from the cover surface of the pyramid, while the

Corresponding Author: Dr. Ahmed A. Hassanain, Agriculture Engineering Department, Faculty of Agriculture, Suez-Canal University, Ismailia, 42552 Egypt

daily yield of the single slope still of 30% higher than that of the pyramid in winter and 3% higher in summer was performed.

The slope of solar still cover on the production rate was investigated by El- Iraqui [8] for Ismailia, Egypt. Three different angles were investigated. Solar still with inclination angle of 20° was found the most efficient slope among the three different inclination angles which were investigated over the summer months.

Solar Still Thermal Analysis: The solar still operation is governed by various heat and mass transfer modes occurring in the system. Within the solar still the following heat transfer modes can be distinguished:

- Convection from water surface to the inner glass cover surface,
- Evaporation from water surface to the inner glass cover surface,
- Radiation from water surface to the inner glass cover surface,
- Convection from basin liner to the water surface,
- Transfer modes from the glass cover to the surrounding environment (radiation and convection, also conduction from the basin bottom to the atmosphere) and finally
- Temperatures mentioned in the analysis are in Kelvin units.

This following analysis based upon the classic work of Cooper [9] and Malik *et al.* [10]. A single basin solar still with energy flow and energy balance equations for the different solar still components can be written as follows according to Abu-Arabi *et al.* [11]:

Heat Balance for the Still Basin (b):

$$m_b C_{pb} \frac{dT_b}{dt} = G A_b - q_{bwb} - q_b \quad (1)$$

Where, C_{pb} is the basin specific heat $Jkg^{-1} K^{-1}$

Heat Balance for Water in the Basin (w):

$$m_w C_{pw} \frac{dT_w}{dt} = G A_w + q_{bwb} - q_{rwb} - q_{cwb} - q_{ewb} \quad (2)$$

Where, C_{pw}: Water specific heat $Jkg^{-1} K^{-1}$

Heat Balance for the Glazing Cover (g):

$$m_g C_{pg} \frac{dT_g}{dt} = G A_g + q_{rwb} + q_{cwb} + q_{ewb} - q_{cga} - q_{rgs} \quad (3)$$

Where, C_{pg}: Glass cover specific heat $Jkg^{-1} K^{-1}$

The Condensate Rate is Given as Abu-Arabi *et al.* [11]:

$$\frac{dm_c}{dt} = \frac{h_{ewb} A_g \left(T_{wb} - T_{gi}\right)}{L_w} = \frac{q_{ewb}}{L_w} \quad (4)$$

q_{cwb} is the rate of the transferred heat by convection in (W) inside the solar still from the water surface to the interior surface of the glass cover is given by Baum and Bairamov [12] in the following equation (5):

$$q_{cwb} = h_{cwb} A_b \left(T_{wb} - T_{gi}\right) \quad (5)$$

Where T_{wb} and T_{gi} are water temperature and temperature of the glass interior surface (K) respectively. Meanwhile, h_{cwb} is the convective heat transfer coefficient in $(Wm^{-2} K^{-1})$; it is given by Dunkle [13] in the following expression:

$$h_{cwb} = 0.884 \left[\left(T_{wb} - T_{gi}\right) + \frac{\left(P_{wb} - P_{gi}\right)}{268900 - P_{wb}} \left(T_{wb}\right)\right]^{1/3} \quad (6)$$

Where P_{wb} and P_{gi} are the partial pressures in (Nm^{-2}) for water vapor at water and the interior glass surface temperatures within the still which are given by Fernandez and Chargoy [14] as:

$$P_{wb} = \exp\left[25.317 - \left(\frac{5144}{T_{wb}}\right)\right] \quad (7)$$

$$P_{gi} = \exp\left[25.317 - \left(\frac{5144}{T_{gi}}\right)\right] \quad (8)$$

The evaporation from the water surface to the interior surface of the glass cover can be estimated as follows:

Rate of the evaporative heat transfer within the still from the water surface to the inner glass cover surface which is denoted by q_{ewb} in (W) units and previously mentioned in equation (3) can be represented as:

$$q_{ewb} = h_{ewb} A_b \left(T_{wb} - T_{gi}\right) \quad (9)$$

Where the evaporative heat transfer coefficient, h_{ewb} in ($Wm^{-2}K^{-1}$), it is given by Abu-Arabi *et al.* [11]:

$$h_{ewb} = 16.273\times10^{-3}\, h_{cwb}\, \frac{\left(P_{wb} - P_{gi}\right)}{\left(T_{wb} - T_{gi}\right)}\, L_w \tag{10}$$

The rate of radiative heat transfer from the water surface to the interior surface of the glass cover, q_{rwb} in (W) in equation (3) is given by:

$$q_{rwb} = h_{rwb}\, A_b \left(T_{wb} - T_{gi}\right) \tag{11}$$

Where h_{rwb} is the radiative heat transfer coefficient in ($Wm^{-2}K^{-1}$), it is given by Abu-Arabi *et al.* [11]:

$$h_{rwb} = \frac{\varepsilon_{eff}\, \sigma \left[\left(T_{wb}\right)^4 - \left(T_{gi}\right)^4\right]}{\left(T_{wb} - T_{gi}\right)} \tag{12}$$

Where ε_{eff} is the effective emissivity factor of diffuse radiation from the water surface to the interior surface of the glass cover and σ is the Stefan-Boltzmann constant taken as $56.7\text{x}10^{-9}$ Wm^{-2} K^{-4} [15]. If the shape factor is taken as the unity and the emissivity of the water is 0.90, the radiative heat transfer from the hot water surface to the interior surface of the glass cover becomes:

$$q_{rwb} = 0.90\, A_b \sigma \left[\left(T_{wb}\right)^4 - \left(T_{gi}\right)^4\right] \tag{13}$$

Thus, the internal heat transfer within the still is governed by three modes. The heat exchange between the condensating and the evaporating surfaces i.e. from the water surface to the interior surface of the glass cover of the solar still which is known as internal heat transfer. These modes are radiation, convection and evaporation and hence the total internal heat transfer coefficient (h_1) from the water surface to the interior surface of the glass cover ($Wm^{-2}K^{-1}$) will be the sum of all these modes heat transfer coefficients according to Tiwari and Tiwari [16], Thus:

$$h_1 = h_{cwb} + h_{ewb} + h_{rwb} \tag{14}$$

Total value of the energy transfer q_1 in (W) within the still from the water surface to the interior surface of the glass cover can be evaluated behind Cooper, [17] as:

$$q_1 = q_{cwb} + q_{ewb} + q_{rwb} \tag{15}$$

The influence of the relative magnitudes of these three modes can be better understood by evaluating the fraction of total energy as done by Cooper [17]. These convective (F_c), evaporative (F_e) and radiative (F_r) fractions which can be evaluated by the following expression [18]:

$$F_c = \frac{q_{cwb}}{q_1} \quad F_e = \frac{q_{ewb}}{q_1} \quad F_r = \frac{q_{rwb}}{q_1} \tag{16}$$

q_{bwb} in (W) in equation (2) which represents the rate of convective heat transfer coefficient from the black basin liner (the hottest region in the still) to the water surface. It is calculated from:

$$q_{bwb} = h_{bwb}\, A_b \left(T_{bi} - T_{wb}\right) \tag{17}$$

Where T_{bi} is the inner basin temperature (K), h_{bwb} is the convective heat transfer coefficient from the black basin liner to the water surface in ($Wm^{-2}K^{-1}$).

The conductive heat transfer coefficient (U_g) (in Wm^{-2} K^{-1} units) through the thickness of the still glass cover (x_g) can be formulated as:

$$U_g = k_g / x_g \tag{18}$$

Where k_g and x_g are the thermal conductivity for the glass cover in (Wm^{-1} K^{-1}) and the glass cover thickness in (m), respectively.

The rate of heat transfer from the exterior surface of the glass cover to the surroundings due to convection, q_{cga} in (W) (caused by the wind):

$$q_{cga} = h_{cga}\, A_g \left(T_{go} - T_{amb}\right) \tag{19}$$

Where T_{go}, T_{amb} and h_{cga} are the outer glass cover temperature, ambient air temperature and convective heat transfer coefficient, respectively. The convective heat transfer coefficient (h_{cga}) depends up on the prevailing wind speed it was given by McAdams [19] as:

$$h_{cga} = 5.7 + 3.8w \tag{20}$$

Where, w is the wind speed in m/s. The rate of the radiative heat transfer from the exterior surface of the glass cover to the sky is given by equation (3):

$$q_{rgs} = h_{rgs} A_g \left(T_{go} - T_{sky}\right) \quad (21)$$

Where h_{rgs} is the radiative heat transfer coefficient in ($Wm^{-2} K^{-1}$); it is given by:

$$h_{rgs} = \frac{\varepsilon_{eff} \sigma \left[\left(T_{go}\right)^4 - \left(T_{sky}\right)^4\right]}{\left(T_{go} - T_{sky}\right)} \quad (22)$$

Where ε_{eff} is the effective emissivity factor of diffuse radiation from the exterior surface of the glass cover to the sky and σ is the Stefan-Boltzmann constant taken as $56.7x10^{-9}$ $Wm^{-2} K^{-4}$. If the shape factor is taken as unity and the emissivity of the glass cover is 0.90, the radiative heat transfer from the exterior surface of the glass cover to the sky becomes:

$$q_{rgs} = 0.90\ \sigma A_g \left[\left(T_{go}\right)^4 - \left(T_{sky}\right)^4\right] \quad (23)$$

Where T_{sky} is the sky temperature and generally the average sky temperature during the operating hours is given by Swinbank [20] i.e.

$$T_{sky} = 0.0552\ T_a^{1.5} \quad (24)$$

The total external heat transfer coefficient (h_2) in $Wm^{-2} K^{-1}$ is given by:

$$h_2 = h_{cga} + h_{rgs} \quad (25)$$

The total value of the rate of energy transfer from the exterior surface of the glass cover to its surroundings q_2 in W can be written as:

$$q_2 = q_{cga} + q_{rgs} \quad (26)$$

Hence, the overall heat transfer coefficient (U_t) through the top of the still can be calculated using the following formula:

$$U_t^{-1} = \left(h_1\right)^{-1} + \left(x_g / k_g\right) + \left(h_2\right)^{-1} \quad (27)$$

The rate of conductive heat losses q_b in (W) from the basin bottom to the atmosphere can be formulated as mentioned by Rai [21] and Hamdan *et al*. [22]:

$$q_b = \frac{k_{in}}{x_{in}} \left(T_{wb} - T_{amb}\right) \quad (28)$$

Where k_{in} and x_{in} are the insulation thermal conductivity in ($Wm^{-1}K^{-1}$) and the basin thickness in (m), respectively. This study aims to investigate single slope solar still, inclined by 20 degree for one direction under the prevailing weather conditions of Egypt. The still characterized by basin that was painted by matt black fiber glass while water inside was kept at 0.5 cm depth (2 liters volume).

MATERIALS AND METHODS

Investigations on an inclined 20° solar still of one direction were carried out under the open environmental conditions at the Agricultural Engineering Department of the Faculty of Agriculture, Suez Canal University, Ismailia, Egypt, throughout the period from 27th of May, 2006 till 26th of December, 2007. The experimental unit's setup is presented schematically in Figure 1. Solar distillation

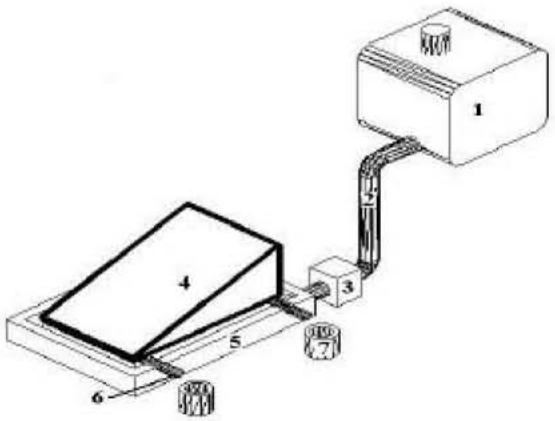

Fig. 1: Set-up for the inclined 20° of one direction (I-20°OD)
1: Preheating feeding tank 2: Feeding plastic hose pipe 3: Water leveling unit 4: Transparent glass cover
5: Water basin 6: Plastic channel 7: Vessel

Table 1: Physical properties for the solar still various components and saline water [24]

Materials	Thermal conductivity,(k), W m^{-1} k^{-1}	Density, (ρ), Kg m^{-3}	Specific heat, (C_p), J kg^{-1} k^{-1}	Thermal diffusivity, (θ), m^2 sec^{-1}
Steel	14.9	7900	477	3.95 x 10^{6}
Glass	0.78	2700	840	3.43 x 10^{-7}
Saline water	0.596	1025	3930	1.47 x 10^{-7}

experimental unit composed three main components: preheating feeding tank, water leveling unit, transparent glazing cover of 6 mm thickness and steel basin. The transparent glazing cover were sealed by silicone rubber sealant to prevent vapor leakage and hot air leakage, since leakage in this area can drastically curtail affects the production rate and because it remains elastic for quite a long time according to Samee *et al.* [23] . Steel basin of 0.80 m long, 0.50 m wide, 0.10 m height and 0.002 m thick were used. Physical properties for the used materials in solar distillation unit are given in Table 1. Within these investigations matt black fiberglass was used as absorbing material type and water depth in the basin was kept at 0.5 cm (i.e. 2 liter). Basin was fed by the Suez Canal saline water. The used saline water within this study has average salinity of 24960 ppm. The unit was fed by the Suez- Canal water from an exact site (region). Physical properties for the saline water are given in Table 1.Two plastic channels were mounted in each basin side with an enough slope to allow the distilled water to run outside the unit in the container. Collected fresh water volume and its salinity were determined.

Methodology

Incident Solar Radiation and Glazing Cover Transmissivity Determination: Mono Crestline solar cell with dimensions of 75 mm by 75 mm a voltage of 0.5 volt and a current of 800 m Ampere was used to determine the global radiation. The short circuit readings that were obtained from the cell were calibrated against apply Pyranometer according to Duffie and Beckman [15] and Mujahed and Almoud [25]. Formula was used to determine the incident solar radiation resulted from a previous calibration against apply Pyranometer. Trails were carried out on a fixed transparent glazing cover of 6 mm. thickness. The glazing cover was divided into cells to determine the glazing cover transmissivity, multiple reading were measured inside and outside the glazing cover for each cell at the same time, the glazing cover transmissivity was found to be 82 % from the incident solar radiation.

Still Productivity and Desalinated Water Salinity Determination: total daily volume of distilled water in liter produced by the still (within a day per unit heat collection area) was determined. Volumes of saline (sea) water and fresh (distilled) water were measured by grading containers. Desalinated water salinity were measured by conductivity meter in ppm (part per million).

Still Performance

Still Efficiency Determination: The experimental steady state efficiency (η) of the solar still calculated from the following equation (29) according to Hamdan *et al.* [22]:

$$\eta = \frac{m L_w}{G A_g \Delta t} \tag{29}$$

Where m, L_w, G, A_g and Δt are the mass condensate and collected in a time interval, water latent heat of evaporation, hourly solar radiation flux, the glass collecting area and the time interval, respectively. Also, the daily efficiency (η_d) was used to determine the solar still efficiency according to Swelam [26] which can be given in the following formula (30):

$$\eta_d = \frac{\Sigma\, m . L_w}{\Sigma\, A . G . t} \tag{30}$$

Equation (30) was used to determine the still daily efficiency, as it is summing up the hourly condensate production (m) multiplied by the latent heat of evaporation (L_w), divided by the summation of the average daily solar radiation (G) the whole still area (A) and time of (t).

The Coefficient of Performance (C.O.P): The coefficient of performance (C.O.P) was determined to investigate the specific design parameter and its effect on the still performance [26]. The C.O.P is an indicator for the still hourly performance. It is given as the following equation (31):

$$COP = \frac{Y . \rho_W . L_W}{G . t} \tag{31}$$

Where, Y: solar still productivity rate $m^3/m^2.sec$, ρ_w water density, kgm^{-3}, L_w; water latent heat of evaporation, $J.kg^{-1}$ and G: solar radiation intensity on the horizontal plane, Wm^{-2}

Wind Speed: The wind velocity is also affecting the glass cover temperature At higher wind velocity the convective heat transfer from the glass cover to atmosphere increases due to increase in convective heat transfer coefficient between glass cover to atmosphere. This effect increases the condensing and evaporation rate and the still productivity according to Yousef and Abu-Arabi [27].

Instrumentations: Data set were taken each two hours around the representative days within the experiments. It includes the measured weather conditions, i.e. global incident solar radiation on a horizontal surface and a tilted surface of glass cover, relative humidity , still productivity and its mass, air temperature inside still, ambient air temperature, basin water temperature, water temperature inside the preheating feeding tank, inner glass cover temperature, outer glass cover temperature, inner basin temperature, outer basin temperature, ground surface temperature, surrounding surface temperature and wind speed.

Global Positioning System: Geographic position system (GPS) GARMIN, eTrex® instrument was used to determine Ismailia region geographic data for the latitude, longitude angles and the altitude from the sea level.

Temperature Measurements: Temperatures inside and outside solar distillation unit were measured by digital thermocouples for the BTC 100 thermocouples which had been previously calibrated against mercury (-10 up to 100 °C) scale thermometer with standard deviation between the thermometers reading of ± 0.47°C.

Relative Humidity: Relative humidity (RH) of the ambient air also the inner air solar distillation unit was measured hourly for the investigation period hours by a means of dry and wet bulb thermometers, which was calibrated previously against a mercury thermometer. Using the psychrometer chart the values of RH were determined.

Wind Speed Measuring Instrument: A TESCO 405-VI Hot Wire Anemometer was used to measure the prevailing wind speeds outside the solar desalination unit.

Desalinated Water Volume and its Salinity: Total soluble salts were Laboratory measured using the conductivity meter (M4310, U.K made by JENWAY LTD). Meanwhile, volumes of saline (sea) water and fresh (distilled) water were simply measured by grading containers.

RESULTS AND DISCUSSIONS

Weather condition throughout the experiments period from 27th of May, 2006 till 26th of December, 2007 were averaged, summarized and presented in Table 2. Due to the obstacles confront the field investigation under the open environmental conditions, the study could not comprise the representative day for the different months that average weather conditions were addressed in Table 2.

Still Temperature Profile: Since sunrise saline water in the basin evaporates where the condensations drops appears at the inner glass cover surface and the glass cover walls this allows the solar radiation (short wavelength) to pass into the solar still mostly absorbed by the blackened base. Water begins to heat up and the moisture content of the air trapped between the water surface and the glass cover. Thus the glass cover traps the solar energy inside the solar still ("greenhouse" effect), the base also radiates energy in the infrared region (long wavelength). In this process the salts and microbes that were in the original water are left behind. When the condensate drops reached certain size they touched each other and flowed under gravity down in zigzag way path and collected. Temperature profile is shown for one day in Fig. 2 for the interior (A) and exterior (B) of the still components around 24 hours on the 27th of May, 2006. Meanwhile, the normalized temperature values for the different still components are shown against the local time in Fig. 3.

From the figures, during the day from sunrise to sunset, the solar radiation and ambient air temperature increased gradually reaching certain maximum values at noon and afternoon by about an hour, respectively and then decreased. The relative humidity behave in the

Table 2: Average weather conditions throughout the field experimental work

Month	Period	Average day length, hour	Air temperature°C	Wind speed, m/sec	Global radiation on horizontal,W/m^2	Global radiation on tilted surface, W/m^2	Relative humidity, %
May	27-29/5/2006	13:54	26.5	0.98	595.8	585	52.6
June	3-27/6/2006	14:03	26.9	0.76	640.1	638.2	49.3
July	2-30/7/2006	13:54	29.5	0.53	601.5	600.7	53.1
August	1:26/8/2006	13:16	29.5	0.42	579.2	580.1	56.1
December	17-26/12/2007	10:13	13.4	0.43	258.1	595.8	64.3

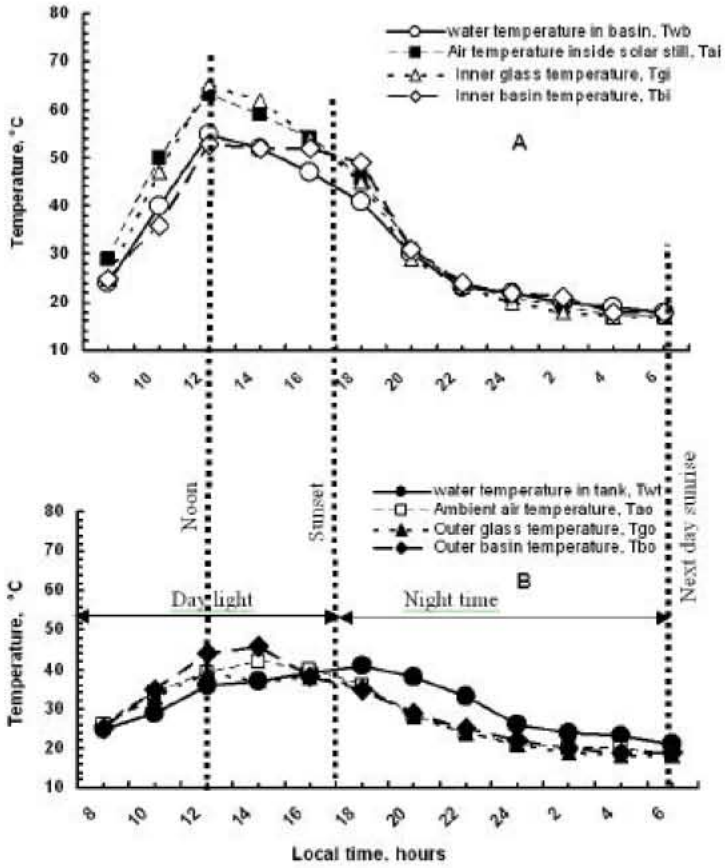

Fig. 2: Temperature profile for the interior (A) and exterior (B) still components measured on 27th May, 2006 for the I-20°OD configuration

reverse way, it decrease during the day reaching certain minimum and then increased again, the wind speed changed in random way. Also, it is observed that, still interior "A" components temperatures were higher than exterior "B" due to existence the glass cover which traps the solar energy inside the solar still ("greenhouse" effect), opaque to the infrared rays from the absorber plate wherever it has heating effect [28] resulted in a higher temperatures inside solar still and existence the wind outside still resulted in a higher convective and radiative heat transfer coefficient which results in a lower glass cover temperature and higher condensation rate inside the solar still and hence a higher yield of the still [29].

From the giving figures it is noticed that, the variation in the solar still components temperatures was high from sunrise till sunset, this refers to the effect of the sun rays on the solar still components. From sunset to the next day sunrise (within night time) temperature the solar still components were nearly has the ambient air temperature. This apart of the preheating feeding tank which performed as a solar water storage tank. Meanwhile, the temperature increase above the ambient air temperature for the preheating feeding tank within the night time was 31, 27.5, 31.1 and 29.8°C for 27th of May, 17th of June, 22nd of July and 26th of August, 2006, respectively.

Still Productivity: Total still productivity in liter/m^2.day for one day from each month was determined i.e. 27th of May, 17th of June, 22nd of July and 26th of August, 2006. The sun-rays incident angle in 27th of May, 17th of June, 22nd of July and 26th of August, 2006 was estimated mathematically from El-Sayed *et al.* [30] to be 13.2°, 10.8°, 11.7° and 22.6° respectively at noon time of the horizontal plan within the investigation on single sloped still angle of 20°.

The still average productivity (P_d) determined according to Swelam, [26] and was found to be 0.0055, zero, 0.102 and 0.317 liter/m^2.day for May, June, July and August, 2006, respectively.

The still average productivity (P_d) for all investigated days of June month was found due to the increase average incident solar radiation throughout this month

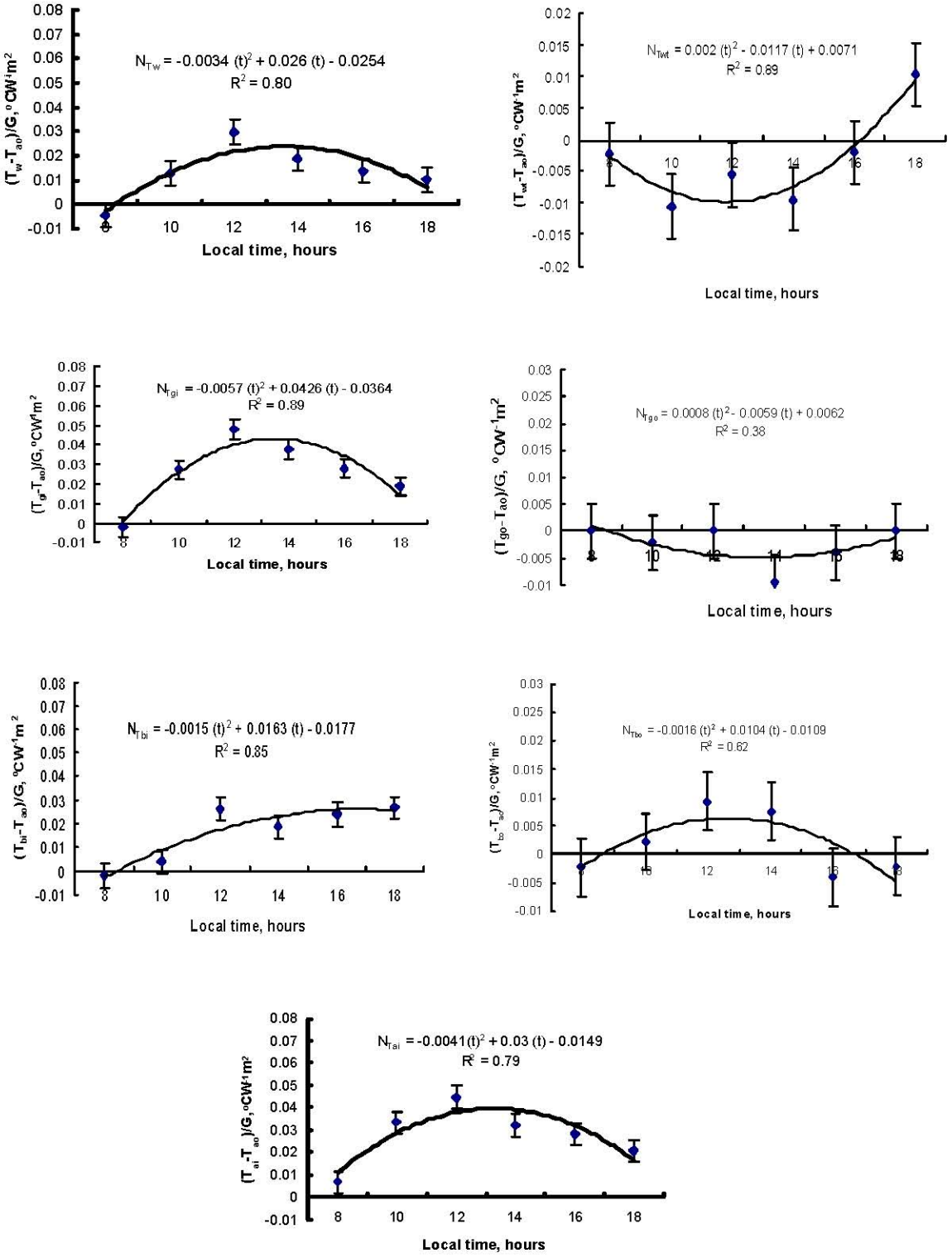

Fig. 3: Normalized temperature values for the different still components against local time on 27th May, 2006

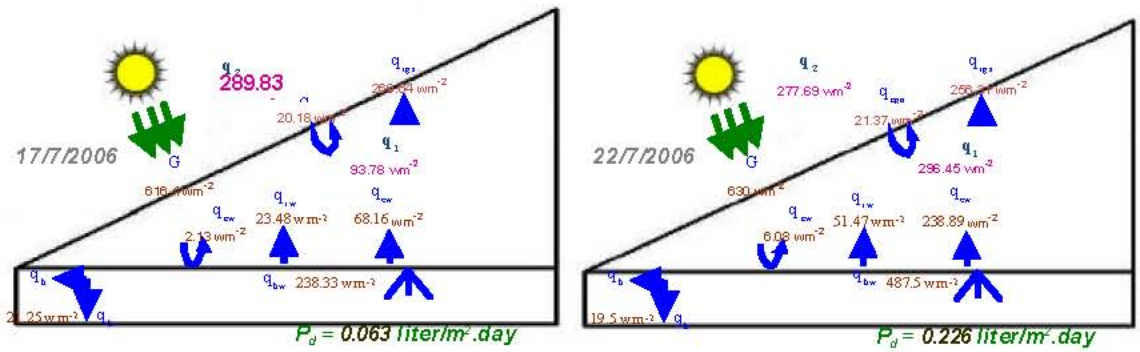

Fig. 4: Still productivity for two days as affected by the thermal and environmental conditions

Table 3: Average still productivity (liter/m^2.day) for some days of each month for I-20°OD configuration

Month	May	July	August	December
Still productivity, lit./m^2.day	0.006	0.12	0.32	0.022

Table 4: Monthly average efficiency for I-20°OD configuration under the open environmental conditions

Month	May	July	August	December
Efficiency, %	0.73	15.3	43.2	9.6

Table 5: Still C.O.P for I-20°OD configuration under the open environmental conditions

Month	May	July	August	December
C.O.P	0.00024	0.003	0.0143	0.0032

Table 6: Average computed thermal values inside and outside solar still under open environmental conditions

Month	Day	Q_{cw}, $Wm^{-2}_{(A)}$	Q_{ew},$Wm^{-2}_{(B)}$	Q_{rw},$Wm^{-2}_{(C)}$	Q_1,$Wm^{-2}_{=(A)+(B)+(C)}$	Q_{cg}, $Wm^{-2}_{(D)}$	Q_{rg}, $Wm^{-2}_{(E)}$	Q_2, $Wm^{-2}_{=(D)+(E)}$	Q_{bw} Wm^{-2}	Q_b Wm^{-2}
May	27/5/2006	9.18	537.76	65.59	612.54	13.06	241.55	254.61	260	12.75
	29/5/2006	12.14	571.18	81.83	665.1	16.62	241.7	258.33	260	13.25
June	3/6/2006	12.83	559.39	87.65	659.88	15.43	253.63	269.07	335.83	10
	5/6/2006	5.684	182.01	43.99	231.6	19	257.66	276.66	227.5	8.75
	10/6/2006	8.27	307.55	62.03	377.86	8.31	235.66	243.97	260	13.75
	12/6/2006	4.62	139.24	41.28	185.15	19	219.79	238.79	260	12
	17/6/2006	6.15	199.59	49.79	255.54	24.93	250.35	275.28	260	16.75
	19/6/2006	6.66	257.78	53.01	317.46	24.93	228.04	252.97	249.16	11.5
	25/6/2006	10.89	553.30	73.27	637.47	15.43	243.74	259.18	693.33	8.5
	27/6/2006	7.15	315	54.57	376.73	9.5	252.64	262.14	682.5	11.75
July	2/7/2006	8.36	378.85	62.98	450.20	45.12	221.20	266.32	769.16	5.75
	4/7/2006	5.68	272.68	48.52	326.89	17.81	256.46	274.27	671.66	15
	9/7/2006	6.06	260.92	50.99	317.98	24.93	255.22	280.15	769.16	15.25
	11/7/2006	6.33	322.15	52.18	380.67	26.12	250.54	276.67	574.16	15.5
	15/7/2006	7.10	332	54.83	393.95	14.25	258.36	272.61	520	16
	17/7/2006	2.13	68.16	23.48	93.78	20.18	269.64	289.83	238.33	21.25
	22/7/2006	6.08	238.89	51.47	296.45	21.37	256.31	277.69	487.5	19.5
	24/7/2006	6.60	311	53.55	371.15	19	258.62	277.62	487.5	18
	30/7/2006	7.17	349.01	55.44	411.62	22.56	258.83	281.39	595.83	16.5
August	1/8/2006	6.96	344.21	54.33	405.52	27.31	260.11	287.42	639.16	15.5
	6/8/2006	5.80	284.44	49.18	339.43	40.37	273.12	313.50	671.66	20
	8/8/2006	5.42	256.99	46.17	308.59	24.93	268.08	293.02	595.83	17.5
	13/8/2006	10.13	424.30	73.55	507.98	30.87	269.02	299.90	595.83	18.25
	15/8/2006	8.48	496.59	65.21	570.29	39.18	293.48	332.66	639.16	25.25
	20/8/2006	8.88	512.79	65.30	586.98	26.12	268.31	294.43	552.5	14.75
	22/8/2006	9.61	588.08	70.98	668.67	29.68	269.19	298.88	541.66	17.25
	26/8/2006	8.7	447.01	65.50	521.22	35.62	274.31	309.93	715	17.5
December	17/12/2006	1.90	34.21	18.80	54.92	9.5	220.97	230.47	119.16	11.5
	18/12/2006	2.48	34.31	23.22	60.01	20.18	220.65	240.83	108.33	13
	21/12/2006	6.82	166.10	49.17	110.11	19	221.74	240.74	314.16	5.5
	22/12/2006	3.81	49.55	33.51	86.89	9.5	221.31	230.81	65	12.25
	26/12/2006	4.23	65.7	34.59	104.56	35.62	243.68	279.31	173.33	15.25

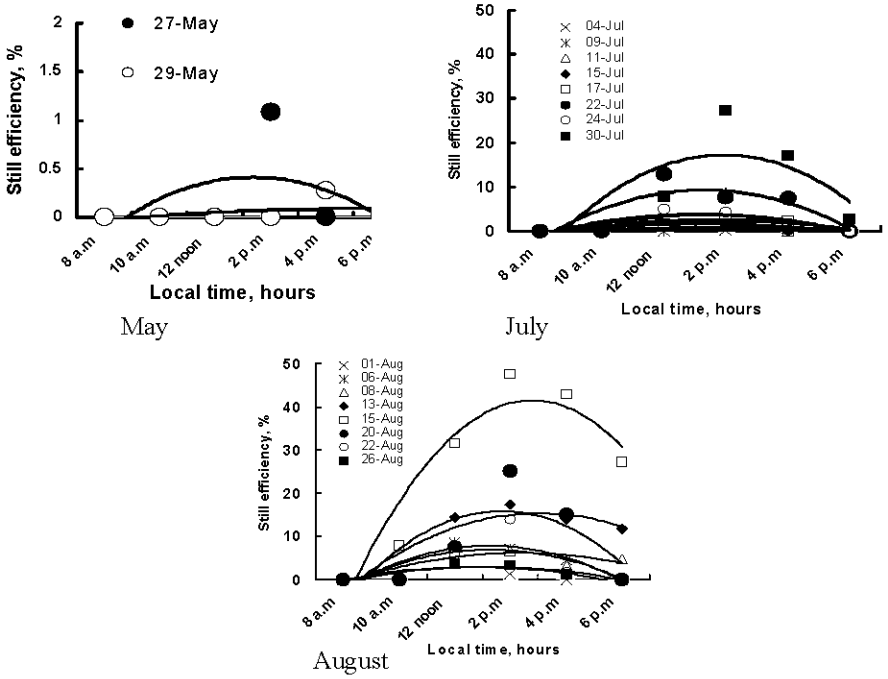

Fig. 5: Still efficiency within different days for different months

comparing to other investigated months as it can be seen from the represented data in Table 2. Increasing the solar radiation caused an overheating the glass cover as a result of absorbs part of the incident solar radiation also it receives all energy transferred by the water vapor during condensation in addition to different heat flows (by convection, radiation and evaporation) going up to the glass as it is given in the mathematical formula. Temperature changes was found slow this may be due to the important heat loss by convection essentially i.e. from the glass to the external environment.This effect is shown for two different days in Fig. 4.

The still productivity as well as the average still efficiency were increased by increasing the average solar radiation. This concept showed complete agreement with at the obtained results at the 22nd of July, 2006 where the still gave the highest productivity of 0.226 liter/m^2.day under average solar radiation of 630 Wm^{-2} while in 27th of May, 2006 the still gave lowest productivity of 0.009 liter/m^2.day under average solar radiation of 611Wm^{-2} according to the average efficiency.

Still Performance

Still Efficiency: Table 4 represents the total still efficiency for the outdoor investigations using equation (30) according to Swelam [26]. Still efficiency within the investigated days is shown in Fig.5 from sunrise to sunset. The still efficiency increased gradually from the sunrise time till it reaches certain maximum value at noon and afternoon by about an hour respectively and then decreased until reached to minimum value at sunset time.

Coefficient of Performance C.O.P.: The average coefficient of performance for the I-20°OD configuration investigated in the open environmental conditions is presented in Table (5).

Solar Still Thermal Analysis: The evaporative heat transfer (Q_{ew}) which was selected as an indicator for the I-20°OD still productivity are shown in Fig. 6 for the investigated I-20°OD configuration versus the day time for different months. From the figure it is noticed that (Q_{ew}) for all selected days represented normal increasing with the incident solar energy I ncrease i.e. from the sunrise to the sunset. The computed thermal analysis for the previously mentioned equations are summarized and represented in Table (6) for the I-20°OD configuration under prevailing weather conditions given in Table 2 for the investigation site.

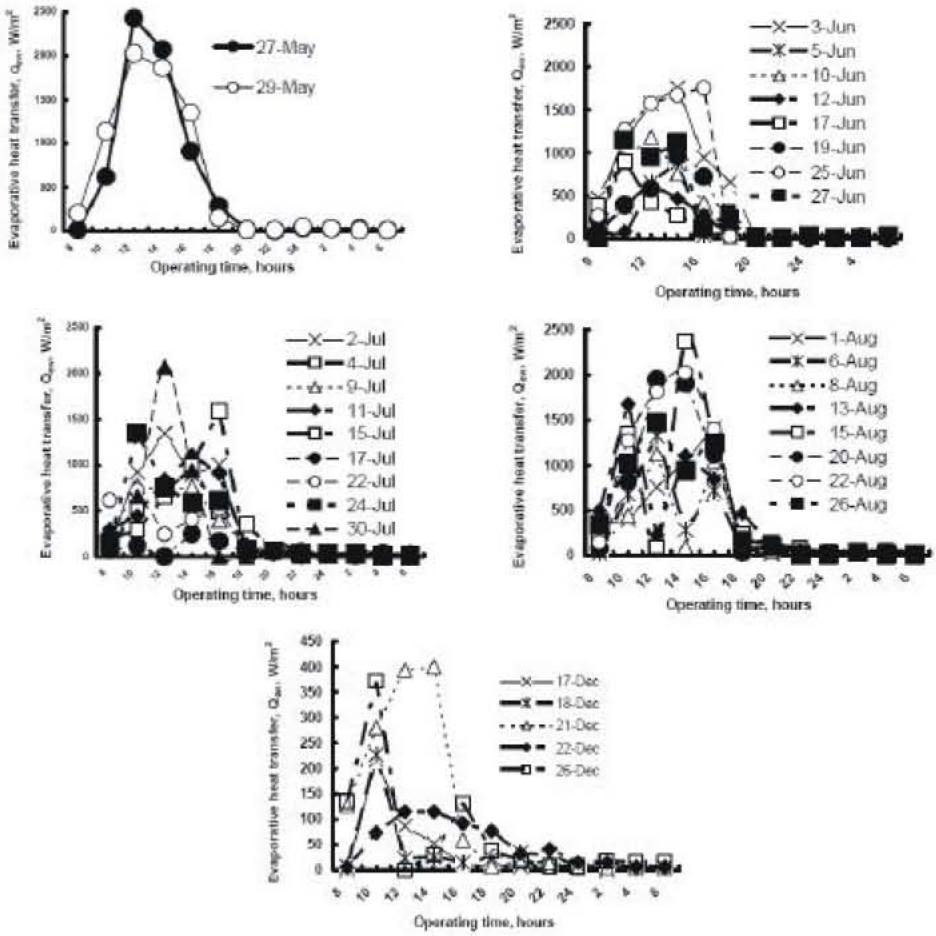

Fig. 6: Evaporative heat transfer (Q_{ew}) computed under open environmental conditions

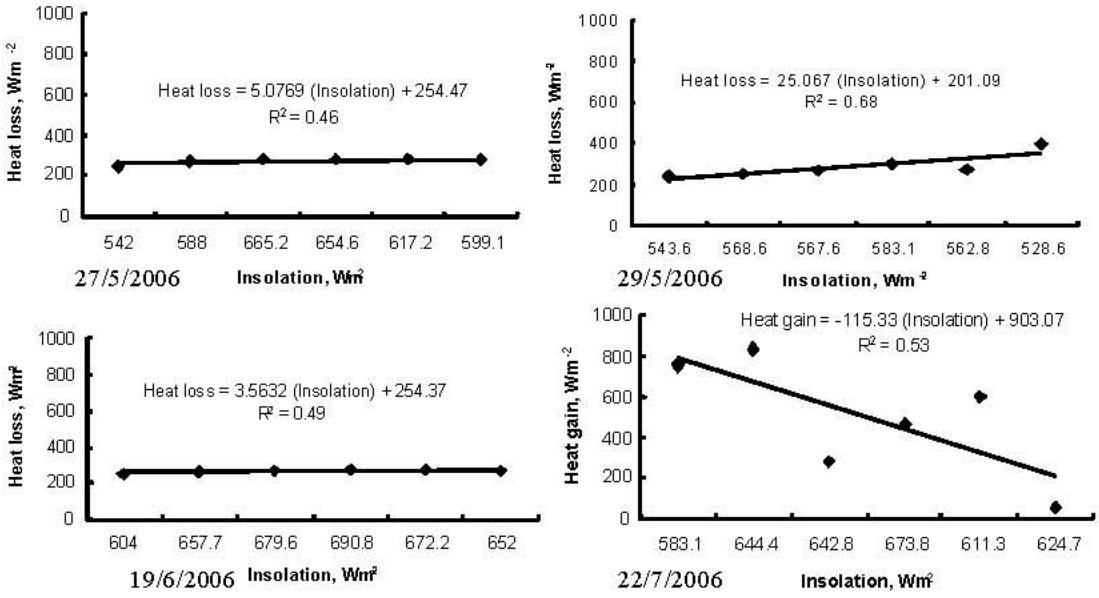

Fig. 7: Relationship between the incident solar radiation in W/m^2 and heat losses per square meter form I-20°OD on different days

In most days when the $Q_1<Q_2$ the still productivity was found zero this is remarkable notice in June month, for instance on 5/6/2006, 12/6/2006 and 17/6/2006 the amount of computed Q_1 were found to be 231.6, 185.15 and 255.54 Watt obtained from each square meter. Meanwhile Q_2 lost from the still toward the surrounding environment were found to be 276.66, 238.79 and 275.28 Watt from the square meter from the still surface area (glazing cover) for the same days respectively. This was reflected on the still productivity which were found null for these days.

Relationships between the incident solar radiation in W/m^2 and heat losses per square meter are presented in Fig. (7) for different days with the obtained equations from the linear fitting lines.

CONCLUSIONS

The study conducted to the highest:

- The highest average distillate production from I-20°OD configuration with matt black fiberglass as an absorbing material occurred in August month where produced 0.317 liter/m^2.day comparing with May and July month where produced 0.0055 and 0.102 liter/m^2.day respectively while the still average productivity (P_d) in June month was found to be zero due to overheating of the glass cover because of increasing the incident solar radiation.

NOMENCLATURE

A_b	Basin area	m^2
A_g	surface area for the glass cover	m^2
A_w	Water surface area	m^2
m_b	Basin mass	kg
m_c	Mass of condensate water	kg
m_g	Mass of the glass cover	kg
m_w	Water mass	kg
n	Day number of the year	
q_{rgs}	Rate of the radiative heat transfer from the exterior surface of the glass cover to the sky	W
T_{ai}	Air temperature inside still	°C
T_{ao}	Air temperature outer still	°C
T_{bo}	Outer basin temperature	°C
T_{gr}	Ground temperature	°C
T_S	Surrounding objects temperature	°C
T_{wt}	Water temperature inside preheating feeding tank	°C
Δt	Time interval	Sec
Latin Symbols		
τ	Transmissivity	%
θ	Thermal diffusivity	$m^2.sec^{-1}$

REFERENCES

1. Seibert, U., G. Vogt, C. Brennig, R. Gebhard and F. Holz, 2004. Autonomous desalination system concepts for sea water and brackish water in rural areas with renewable energies-Potentials, Technologies, Field Experience, Socio-technical and socio-economic impacts-ADIRA. Paper: Desalination Strategies in South Mediterranean Countries, 30. May-2.June, Marrakech, Morocco.
2. Fahmy, S., M. Ezzat, A. Shalaby, H. El-Atfy, H. Kandil, M. El-Sharkawy, M. Allam, I. Al-Assiouty and A. Tczap, 2002. Water policy review and irrigation study. Ministry and water resources and irrigation and US Agency for international development contract No. PCE-I-00-96.
3. Gocht, W., A. Sommerfeld, R. Rautenbach, Th. Melin, L. Eilers, A. Neskakis, D. Herold, V. Horstmnn, M. Kabariti and A. Muhaidat, 1998. Renewable Energy, 14(1-4): 287-292.
4. Tiwari, G.N., H.N. Singh and R. Tripathi, 2003. Present status of solar distillation. Solar Energy, 75(5): 367-373.
5. Abdenacer, P.K. and S. Nafila, 2007. Impact of temperature difference (water-solar collector) on solar still global efficiency. Desalination, 209: 298-305.
6. Abdel-Ghaffar, E.A.M., 1989. Development of a simple passive solar still suitable for new village's houses at the northern western coast of Alexandria. Proceeding of the Egyptian-German Conference Agricultural Mechanization, 4-6 October, Mansura University, pp: 295-310.
7. Fath, H.E.S., M. El-Samanoudy, K. Fahmy and T. Hassabou, 2001. Thermal- economic analysis and comparison between pyramid-shape and single-slope solar still configurations. Desalination, 159: 69-79.
8. El-Iraqui, M.H.I., 1981. Studies of solar energy with some applications. Master of Science Degree in Physics, Thesis, Suez Canal University.
9. Cooper, P.I., 1970. The transient analysis of a glass covered solar still. Ph.D. thesis, University of Western Australia.
10. Malik, M.A.S., G.N. Tiwari, A. Kumar and M.S. Sodha, 1982. Solar Distillation. Pergamon Press, Oxford, pp: 175.
11. Abu-Arabi, M., Y. Zurigat, H. Al-Hinai and S. Al-Hiddabi, 2002. Modeling and performance analysis of a solar desalination unit with double-glass cover cooling. Desalination, 143: 173-182.
12. Baum, V.A. and R. Bairamov, 1964. Heat and mass transfer processes in solar stills of hot- box type. Solar Energy, 8: 78.

13. Dunkle, R.V., 1961. Solar water distillation: the roof- type still and a multiple- effect diffusion still. International Developments in Heat Transfer, ASME, Proceedings International Heat Transfer, University of Colorado, Part V: 895.
14. Fernandez, J.L. and N. Chargoy, 1990. Multi stage indirectly heated solar still. Solar Energy, Journal, 44(4): 215-223.
15. Duffie, J.A. and W.A. Beckman, 1991. Solar engineering of the thermal processes. Second edition, USA: Wiley.
16. Tiwari, A.K. and G.N. Tiwari, 2007. Thermal modeling based on solar fraction and experimental study of the annual and seasonal performance of a single slope passive solar still: The effect of water depths. Desalination, 207: 184-204.
17. Cooper, P.I., 1973. Digital simulation of experimental solar still data. Solar Energy, 14: 451.
18. Sartori, E., 1996. Solar still versus solar evaporator: A comparison study between their thermal behaviors. Solar Energy, 56: 199-206.
19. McAdams, W.H., 1954. Heat Transmission. 3rd ed., McGraw-Hill Book Company, N.Y. USA.
20. Swinbank, 1963. Long-wave radiation from clear skies. Quarterly Journal of the Royal Meteorological Society, pp: 89.
21. Rai, G.D., 1980. Solar energy utilization. A text book for engineering students. Some additional methods of solar energy utilization. Delhi: Khanna; pp: 194-97. [chapter 12].
22. Hamdan, M.A., A.M. Musa and B.A. Jubran, 1999. Performance of solar still under Jordanian climate. Energy Conservation and Management, 40: 495-503.
23. Samee, M.A., U.K. Mirza, T. Majeed and N. Ahmed, 2005. Design and performance of a simple single basin solar still. Renewable and Sustainable Reviews, pp: 1-8.
24. Gebhart, B., 1993. Heat Conduction and Mass Diffusion. McGraw- Hill Inc, New York, pp: 620.
25. Mujahed, A.M. and A.R.M. Almoud, 1988. An easily designed and constructed photovoltaic pyrheliometer. Solar and Wind Technol., 5(2): 127-130.
26. Swelam, A.I., 2005. Engineering Study on Water Desalination, Doctor of Philosophy, Department of Agricultural Engineering, Faculty of Agriculture, Zagazig University, Egypt.
27. Yousef, H. and M. Abu-Arabi, 2004. Modeling and performance analysis of a regenerative solar desalination unit. Applied of Thermal Engineering, 24: 1061-1072.
28. Badran, O.O. and I. Al-Hayek, 2004. The effect of using different designs of solar stills on water distillation. Desalination, 16x (2004) on PROOF DES 2652.
29. Al-Hinai, H., M.S. Al-Nassri and B.A. Jubran, 2002. Effect of climatic, design and operational parameters on the yield of a simple solar still. Energy Conversion and Management, 43: 1639-1650.
30. EL-Sayed, M.M., S.A. Radwan, A.A. Hassanain and S.M. Mosalhi, 2005. Weather on performance of solar module for water pumping. Misr Journal of Agricultural Engineering, 22(3): 874-898.